



Original Article

Gamma spectrum denoising method based on improved wavelet threshold

Bo Xie ^{a, b, d, *}, Zhangqiang Xiong ^{a, b}, Zhijian Wang ^c, Lijiao Zhang ^{c, **,}, Dazhou Zhang ^{a, b}, Fusheng Li ^c^a Hunan Key Laboratory of Nonferrous Resources and Geological Hazards Exploration, Changsha, 410083, China^b School of Geosciences and Info-Physics, Central South University, Changsha, 410083, China^c Engineering Research Center of Nuclear Technology Application, East China University of Technology, Ministry of Education, Nanchang, 330013, China^d School of Information engineering, East China University of Technology, Nanchang, 330013, China

ARTICLE INFO

Article history:

Received 14 August 2019

Received in revised form

24 December 2019

Accepted 20 January 2020

Available online 24 January 2020

Keywords:

Gamma spectrum

Denoising

Wavelet threshold

ABSTRACT

Adverse effects in the measured gamma spectrum caused by radioactive statistical fluctuations, gamma ray scattering, and electronic noise can be reduced by energy spectrum denoising. Wavelet threshold denoising can be used to perform multi-scale and multi-resolution analysis on noisy signals with small root mean square errors and high signal-to-noise ratios. However, in traditional wavelet threshold denoising methods, there are signal oscillations in hard threshold denoising and constant deviations in soft threshold denoising. An improved wavelet threshold calculation method and threshold processing function are proposed in this paper. The improved threshold calculation method takes into account the influence of the number of wavelet decomposition layers and reduces the deviation caused by the inaccuracy of the threshold. The improved threshold processing function can be continuously guided, which solves the discontinuity of the traditional hard threshold function, avoids the constant deviation caused by the traditional soft threshold method. The examples show that the proposed method can accurately denoise and preserves the characteristic signals well in the gamma energy spectrum.

© 2020 Korean Nuclear Society, Published by Elsevier Korea LLC. This is an open access article under the CC BY-NC-ND license (<http://creativecommons.org/licenses/by-nc-nd/4.0/>).

1. Introduction

In gamma spectrometry, owing to the influence of radioactive statistical fluctuations, gamma ray scattering, and electronic noise, the measured energy spectrum data has a certain random distribution [1,2]. This random distribution adversely affects the processing of subsequent energy spectrum data such as peak position determination, net peak area calculation, and background subtraction [3–5]. To accurately and qualitatively quantify the energy spectrum, it is first necessary to denoise the energy spectrum data. Commonly used gamma energy spectrum denoising methods include the arithmetic sliding average method, the center of gravity method, and the wavelet threshold

denoising method [6–10]. Among these methods, wavelet threshold denoising exhibits satisfactory local characteristics in both the time and frequency domains; it can be used for multi-resolution analysis. Moreover, it is highly suitable for the analysis and denoising of abrupt signals and has several practical applications such as image denoising [11–13], biomedical signal processing [14,15], Energy spectrum signal denoising [16–19], etc. Many studies have shown that the energy spectrum signals denoised by the wavelet threshold have a higher signal-to-noise ratios (SNRs) and smaller root mean square errors (RMSEs) and can better preserve the characteristic signals compared to other denoising techniques [20–22]. Commonly used wavelet threshold denoising methods include hard threshold denoising and soft threshold denoising. However, following energy spectrum signal reconstruction using hard threshold denoising, the signal oscillation phenomenon (pseudo Gibbs phenomenon) occurs, which causes discontinuity in the energy spectrum; Furthermore, there is constant deviation in the reconstructed energy spectrum signals denoised using the soft threshold; thus, their approximations are less accurate [23–26]. Therefore, based

* Corresponding author. Hunan Key Laboratory of Nonferrous Resources and Geological Hazards Exploration, Changsha, 410083, China.

** Corresponding author: Engineering Research Center of Nuclear Technology Application, East China University of Technology, Ministry of Education, Nanchang, 330013, China

E-mail addresses: 40252126@qq.com (B. Xie), 405179625@qq.com (Z. Xiong).

on the traditional wavelet threshold denoising principle, this paper proposes a new threshold calculation method and threshold processing function, which are used to denoise gamma spectroscopy data. Finally, to prove the superiority of the proposed method, its results are compared with those obtained using the five-point arithmetic average method, the five-point centre-of-gravity method, and the traditional wavelet hard and soft threshold denoising methods.

2. Wavelet threshold denoising: principle and steps

Measured gamma spectra can be considered mixed spectra composed of low-frequency real energy spectra and high-frequency noise:

$$f_i = s_i + x_i \quad i = 1, 2, \dots, N, \tag{1}$$

where f_i is the measured gamma energy spectrum, s_i is the real gamma energy spectrum, x_i is the noise signal, i is energy channel, and N is the signal length.

Wavelet threshold denoising uses the feature that noise is usually in the high-frequency band. The threshold is processed by the decomposed wavelet high-frequency coefficients, and then the inverse wavelet transform is used to reconstruct the signal to remove high-frequency noise.

The main steps of wavelet threshold denoising are as follows:

- 1) Select a suitable wavelet basis function and number of decomposition layers to perform multi-scale decomposition on f_i ;
- 2) Design a threshold calculation method and threshold processing function;
- 3) Use the threshold value obtained in the second step and the threshold processing function to limit the wavelet coefficients obtained in the first step;
- 4) Reconstruct the energy spectrum information.

3. Wavelet threshold denoising

3.1. Wavelet basis function

There are many wavelet basis functions that can be used for threshold denoising [27–29]. Table 1 lists the characteristics of some commonly used wavelet basis functions.

Considering the various characteristics of a wavelet basis function, combined with the characteristics of a large number of mutated signals in gamma spectroscopy data, Daubechies, Symlets, Coiflets, and other three series of wavelets can be used. To select the optimal wavelet basis function, wavelet threshold denoising is performed using different wavelet basis functions, and the SNRs and RMSEs of the reconstructed gamma spectrum signals after denoising are compared, as shown in Table 2. Based on the results of Table 2, we selected the sym6 wavelet basis function (see

Table 2

Signal-to-noise ratio and root mean square error of the energy spectrum signals after denoising using various wavelet basis functions.

Wavelet basis function	SNR	RMSE	Wavelet basis function	SNR	RMSE
Sym4	43.03	5.37	DB6	42.90	5.45
Sym5	42.93	5.43	DB7	42.37	5.79
Sym6	43.22	5.20	DB8	42.76	5.54
Sym7	41.63	6.31	Coif2	42.35	5.80
Sym8	42.45	5.73	Coif3	42.71	5.57
Db4	42.08	5.99	Coif4	43.23	5.24
Db5	42.68	5.52	Coif5	43.31	5.19

Table 3

Denoising effect evaluation of Gaussian signal with white noise.

Denoising Methods	S	SNR	RMSE
Five-point arithmetic average	1.32	27.39	5.15
Five-point center of gravity	1.67	23.69	7.88
Hard threshold	0.58	28.74	4.41
Soft threshold	0.82	29.52	4.03
New threshold	1.01	29.49	4.04

Table 3).

3.2. Wavelet threshold

The wavelet threshold has a great influence on the denoising effect. When the threshold is too small, denoising may be incomplete and interference information may remain; when the wavelet threshold is too large, useful information may be lost. At present, the unified threshold is widely used [30,31], which is based on the Gaussian noise model and is derived from independent normal variable decision theory:

$$\lambda = \sigma\sqrt{2 \ln N} \tag{2}$$

where N is the signal length and σ is the standard deviation in the noise.

In practical applications, the signal length N is fixed for a particular detector; however, the noise standard deviation σ needs to be estimated; this is commonly carried out using the following equation:

$$\sigma = \frac{\text{median} [|d_j(k)|]}{0.6745} \tag{3}$$

where j is the wavelet decomposition scale and *median* is the intermediate value function.

The influence of the number of decomposition layers is not considered when Equation (2) is used to calculate the threshold. However, in a wavelet transform, as the number of decomposition layers increases, the noise in the wavelet detail coefficients decreases; thus, the threshold calculated by Equation (2) is not accurate. Moreover, in the gamma energy spectrum, although the

Table 1

Main characteristics of commonly used wavelet basis functions.

Wavelet basis function	Orthogonality	Symmetry	Tight support	Regularity	Vanishing moment order
Haar	yes	Symmetry	yes	yes	1
Daubechies(dbN)	yes	Approximate symmetry	yes	yes	N
Symlets(symN)	yes	Approximate symmetry	yes	yes	N
Coiflets(coifN)	yes	Approximate symmetry	yes	yes	2N
Biorhogonal (biorN _r N _d)	no	Asymmetry	yes	yes	N _r -1

characteristic signals are Gaussian distribution, the noise is not Gaussian white noise [21,22], this effect has a negative impact when unified threshold denoising is applied directly.

When calculating the threshold using Equation (2), a coefficient μ is additionally introduced. Thus, the threshold decreases with an increase in the number of decomposition layers. The influence of noise standard deviation and the number of decomposition layers of the wavelet transform on the calculated threshold is considered as

$$\mu = 1 / \ln(i^2 + 1) \quad (4)$$

where i is the number of decomposition layers of the wavelet transform.

The new threshold calculation function is as follows:

$$\lambda = \mu \cdot \sigma \sqrt{2 \ln N} \quad (5)$$

3.3. Threshold processing function

Threshold processing is the embodiment of a multi-wavelet coefficient processing strategy, which is a key step in wavelet threshold denoising. Current commonly used threshold processing functions have hard and soft threshold processing functions [30,31].

1) Hard threshold processing

When the absolute value of the wavelet coefficient is less than a given threshold, the coefficient is set to 0, and when the absolute value is greater than the threshold, its original value is retained. This function can be expressed as

$$C_\lambda = \begin{cases} C, & |C| \geq \lambda \\ 0, & |C| < \lambda \end{cases} \quad (6)$$

where C is the wavelet coefficient, λ is the threshold value, and C_λ is the wavelet coefficient after threshold processing.

2) Soft threshold processing

When the absolute value of the wavelet coefficient is less than a given threshold, the coefficient is set to 0. When the absolute value is greater than the threshold, the threshold is subtracted from the original value. This function is expressed as

$$C_\lambda = \begin{cases} \text{sign}(C)(|C| - \lambda), & |C| \geq \lambda \\ 0, & |C| < \lambda \end{cases} \quad (7)$$

Hard threshold processing only retains large wavelet coefficients; it sets the small wavelet coefficients to zero and exhibits discontinuity. Following signal reconstruction, oscillations (pseudo-Gibbs phenomenon) occur, which causes loss in the continuity of the spectrum.

The smaller wavelet coefficients are set to zero by the soft threshold processing; it also reduces the larger wavelet coefficients to zero. Although the processed wavelet coefficients exhibit a good overall continuity, there is a constant deviation, resulting in reconstructed signals and originals. The signal approximation is reduced.

3) Improved threshold

Addressing the shortcomings of traditional hard and soft thresholds, this paper proposes an improved threshold processing

strategy to smoothen the measured gamma spectroscopy data. The improved threshold function is as follows:

$$C_\lambda = \begin{cases} \text{sign}(C) \left(|C| - \frac{\lambda}{e^{\sqrt{(|C|)^2 - \lambda^2}}} \right), & |C| \geq \lambda \\ 0, & |C| < \lambda \end{cases} \quad (8)$$

The new threshold function is second-order steerable and exhibits good continuity. When $|C| \rightarrow \lambda$, the characteristics of the soft threshold function are presented; when $|C| \gg \lambda$, the new threshold function considers $y = |C|$ as the asymptote; as $|C|$ continues to increase, C_λ is approaching $|C|$ and exhibiting the characteristics of a hard threshold function. The new threshold function avoids the discontinuity of the hard threshold function and the constant deviation of the soft threshold function.

4. Case analysis

To verify the method proposed in this paper, the measured gamma spectroscopy data are denoised by a five-point arithmetic averaging method, five-point center of gravity method, hard threshold, soft threshold, and new threshold processing method discussed in this paper. The results obtained by various methods are compared in Fig. (1). In the wavelet transform, sym6 is selected as the wavelet basis function, and the number of decomposition layers is 4 (see Fig. 2).

The figure shows that after denoising the original spectrum using the five methods, the main features of the spectrum are constant and the statistical fluctuations in the original spectrum are suppressed. Among them, the five-point arithmetic average and five-point center of gravity methods have a slightly stronger denoising effect; however, noise is still detected at the partial inflection point of the curve (Figs. 1(a), 1(b)). The traditional soft threshold and new threshold denoising methods discussed in this paper have obtained a smoother spectral line and better denoising effect, compared with the other methods. However, there is a deviation in the curve after soft threshold processing (Fig. 1(e)), which may cause partial characteristic signal loss. To further evaluate the effects of the various denoising methods, a quantitative analysis is required. In this study, the smoothness, RMSE, and SNR are employed for this analysis. In the experimental data, the energy spectrum data of the background model are assumed to be noise, and the data of U, Th, K and mixed models are composed of real signals and noise signals.

1) Smoothness

Smoothness describes the smoothness of the line after denoising, generally expressed as the ratio of the variance of the spectral data after noise reduction to the variance of the original spectrum data, as follows:

$$S = \sqrt{\frac{\sum_{k=1}^N [y(k+1) - y(k)]^2}{\sum_{k=1}^N [f(k+1) - f(k)]^2}} \quad (9)$$

where f is the original energy spectrum data; y is the denoised energy spectrum data; k is the channel address; and N is the number of sampling points. The smaller is the S value, the smoother is the line and the better is the denoising.

2) Signal-to-noise ratio

The SNR describes the ratio between the signal and the noise. The larger its value, the better the denoising effect.

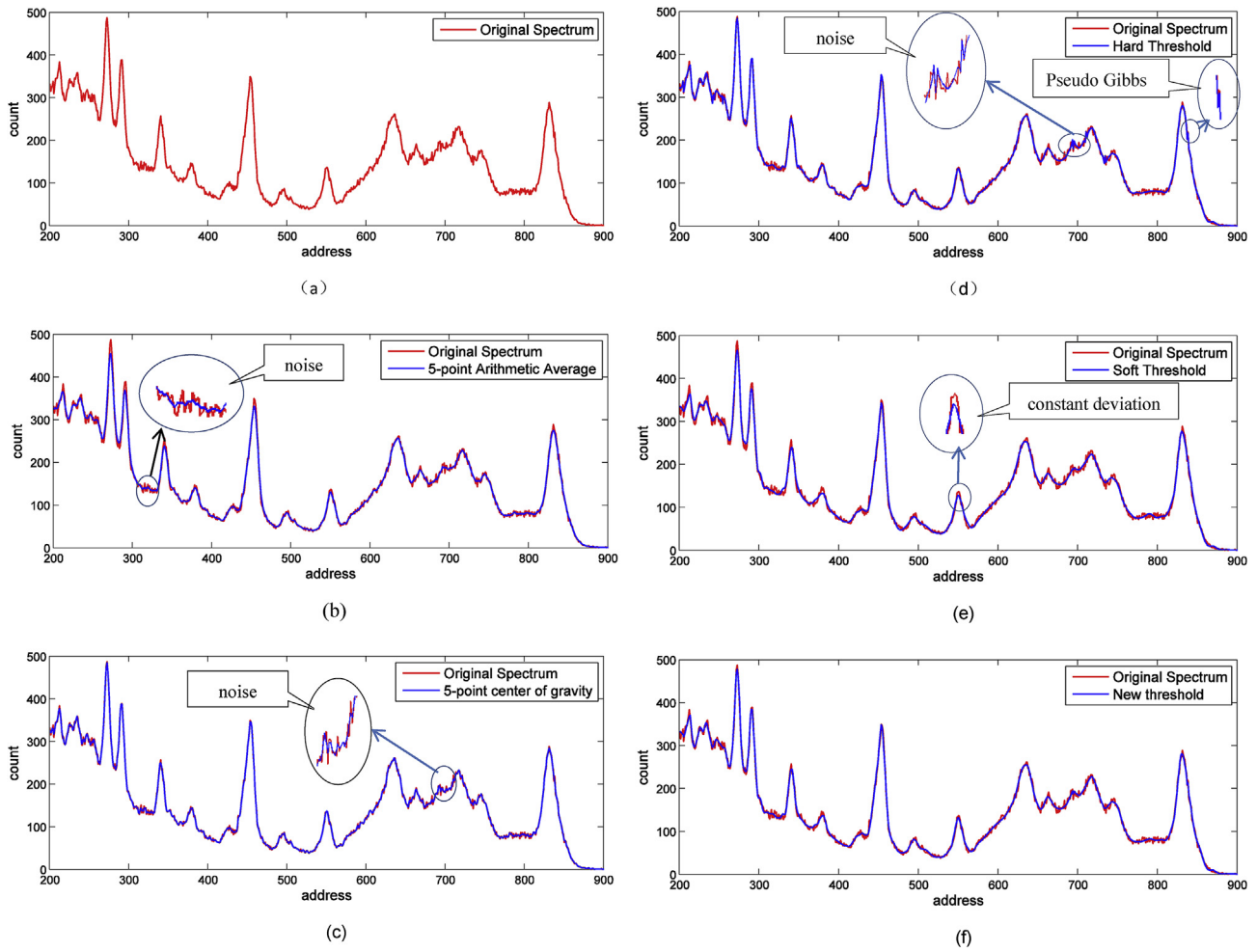


Fig. 1. Comparison of five denoising methods: (a) measured gamma spectroscopy; (b) five-point arithmetic average; (c) five-point center-of-gravity; (d) hard threshold; (e) soft threshold; and (f) improved threshold.

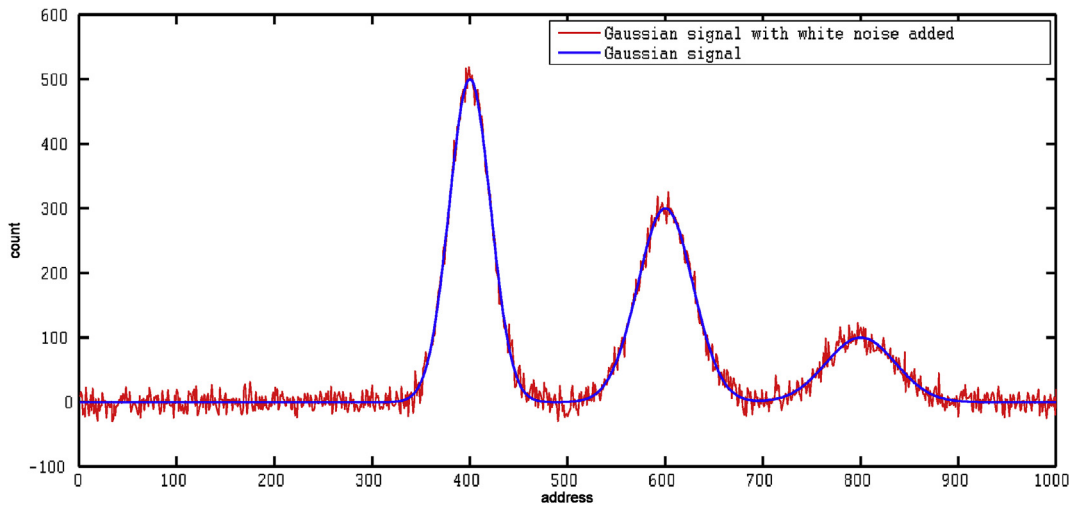


Fig. 2. Gaussian signal.

$$SNR = 10 \log \frac{\sum_{k=1}^N f^2(k)}{\sum_{k=1}^N [f(k) - y(k)]^2} \quad (10)$$

3) Root mean square error

The RMSE can be used to measure the difference between the denoised signal and the real signal by reflecting the square root of the mean of the squared deviation of the reconstructed signal from the original signal. The smaller the value, the closer the denoised signal is to the real signal, and the better is the denoising effect. The RMSE expression is as follows:

$$RMSE = \sqrt{\frac{1}{N} \sum_{k=1}^N [f(k) - y(k)]^2} \quad (11)$$

In order to evaluate the denoising effect of the methods studied more accurately, first a Gaussian signal with three characteristic peaks added with white noise is simulated. The function of the Gaussian signal is as follows:

$$S(x) = a_1 e^{-\frac{(x-b_1)^2}{2c_1^2}} + a_2 e^{-\frac{(x-b_2)^2}{2c_2^2}} + a_3 e^{-\frac{(x-b_3)^2}{2c_3^2}} \quad (12)$$

In the function, x is channels of the signal, $x = 1, 2, \dots, 1000$; a is the peak count, $a_1 = 500, a_2 = 300, a_3 = 100$; b is the number of channels where the peak is located, $b_1 = 400, b_2 = 600, b_3 = 800$; c is the standard deviation, $c_1 = 30, c_2 = 40, c_3 = 50$. white noise with a signal-to-noise ratio of 30 ($SNR = 30$) to the signal is added as follows:

The noisy signals are denoised using the five methods studied, the results of above three indications are as follows:

From the results, the new method discussed in this paper has the best smoothness, which is close to 1. Compared with the traditional method, the SNR of the three wavelet transforms has been improved. The soft-threshold denoising and the new threshold denoising have the highest signal-to-noise ratio. Compared with the traditional method, the three wavelet transforms of the RMSE are smaller.

In order to further verify the denoising effect of the research method, the measured signal obtained from the standard model was used for quantitative analysis to evaluate the effect of the research method in practical application. The measured data are U, Th, K and mixed models of a model station in China. The quantitative analysis results are as follows:

The quantitative evaluation of the five energy spectrum smoothing methods is shown in Tables 4–7. As shown in Tables 4–7, the five-point arithmetic average method exhibits the lowest smoothness, suggesting that the smoothness of the line after processing is the best; in contrast, the five-point center of gravity method exhibits the highest smoothness, suggesting that the smoothness of the line is the worst after processing. The three

Table 4
Energy spectrum denoising effect evaluation of mixed model.

Denoising Methods	S	SNR	RMSE
Five-point arithmetic average	0.60	16.47	114.14
Five-point center of gravity	1.56	33.17	16.69
Hard threshold	1.07	44.48	4.54
Soft threshold	0.99	39.13	8.40
New threshold	1.01	42.80	5.52

Table 5
Energy spectrum denoising effect evaluation of K model.

Denoising Methods	S	SNR	RMSE
Five-point arithmetic average	0.62	16.68	24.23
Five-point center of gravity	1.53	33.42	3.53
Hard threshold	1.05	33.56	3.47
Soft threshold	0.98	30.96	4.68
New threshold	1.02	32.62	3.87

Table 6
Energy spectrum denoising effect evaluation of U model.

Denoising Methods	S	SNR	RMSE
Five-point arithmetic average	0.62	16.69	24.23
Five-point center of gravity	1.53	33.42	3.53
Hard threshold	1.05	33.55	3.47
Soft threshold	0.98	30.96	4.68
New threshold	1.02	32.62	3.87

Table 7
Energy spectrum denoising effect evaluation of Th model.

Denoising Methods	S	SNR	RMSE
Five-point arithmetic average	0.64	17.77	110.0
Five-point center of gravity	1.47	34.41	16.19
Hard threshold	1.06	43.98	5.38
Soft threshold	0.99	39.47	9.05
New threshold	1.01	42.21	6.60

wavelet threshold denoising methods are all around 1.0. The smoothness value of improved threshold method is close to the smoothness value obtained by the traditional soft threshold method; however, it is improved compared with the traditional hard threshold.

In Tables 4–7, the arithmetic-average and center of gravity methods have relatively low SNRs, and the denoising effects are poor, while the three wavelet threshold denoising methods have relatively high SNRs. The improved threshold denoising method exhibits an SNR close to that of the hard threshold method and is improved relative to the soft threshold method. The difference between the SNR values is low, indicating that the denoising effects of the three wavelet threshold methods are all good.

RMSE can be used to describe the difference between the real signal and the processed signal. The RMSEs of the five-point center of gravity and five-point arithmetic average methods are large, indicating that the denoised and real signals are generated by the two methods and exhibit large deviations. The root mean square errors of the hard threshold method, soft threshold method, and new threshold method are all small, indicating that the energy spectrum after denoised by the three wavelet transforms is closer to the real signal. The RMSE is relatively large, and the processed characteristic signal is also quite different from the original curve, indicating that there is a constant deviation in the soft threshold denoising method. The traditional hard threshold and improved threshold methods exhibit a smaller RMSE and better preserve the characteristic signals in the spectral data.

In summary, the following conclusions can be drawn from the energy spectrum smoothing results of models:the improved threshold denoising method has higher SNR and smaller RMSE compared with the arithmetic-average and center of gravity methods; further, it exhibits higher similarity with the original energy spectrum signal. Compared with hard threshold denoising method, the improved threshold denoising method avoids the pseudo Gibbs phenomenon and improves the smoothness of the

denoised line; compared with the soft threshold denoising method, it avoids the constant deviation of the data after denoised, thus, improving the SNR and reducing the RMSE.

5. Conclusions

In this study, an improved threshold calculation method and threshold processing function are analyzed to denoise the gamma energy spectrum. Through theoretical research and experimental analyses, the following conclusions can be drawn:

- 1) Compared with the traditional arithmetic average and center of gravity methods, the improved threshold denoising method exhibits a smaller RMSE and higher SNR, which retains the advantage of wavelet threshold denoising;
- 2) The improved threshold calculation method considers the influence of the number of decomposition layers; hence, the calculated threshold is more accurate and useful signals are not lost during denoising;
- 3) The improved threshold processing function avoids the pseudo-Gibbs phenomenon in the hard threshold method. Compared with the traditional soft threshold method, the improved threshold processing function further reduces the RMSE, improves the SNR. It also avoids the constant deviation, so the characteristic signals are preserved well.

Declaration of competing interest

The authors declared that they have no conflicts of interest to this work.

Acknowledgments

This research received no external funding. The authors would like to acknowledge the Institute of Nuclear Application of ECUT in providing data.

References

- [1] C. Liu, W. Zhang, D. Pierce, K. Ungar, C. Tulk, M. Bean, Gamma spectrum and coincidence summation simulations with Geant4 in the analysis of radionuclide using BEGe detector, *Appl. Radiat. Isot.* 137 (2018) 210–218.
- [2] F.A. Maya, Riyatun Suharyana, K. Azizul, Neutron and gamma energy spectrum of the subcritical assembly for 99Mo production (SAMOP), *J. Phys. Conf.* 1153 (2019).
- [3] W. Hou, Z.W. Liu, H. Zhou, F.X. Liang, R.Z. Zhang, Study of the False Peak Eliminating Algorithm in Fine EDXRF, *Spectroscopy and Spectral Analysis* 38 (11) (2018) 3593–3597.
- [4] T. Nemes, D. Mrdja, I. Bikit Slivka, S.K. Bikit, S. Samardzic, Influence of angular correlations on the full energy peak efficiency calibration using the sum peak method, *Nucl. Instrum. Methods Phys. Res. Sect. A Accel. Spectrom. Detect. Assoc. Equip.* 98 (21) (2019) 37–40.
- [5] J. Ordóñez, S. Gallardo, J. Ortiz, M. Sáez-Muñoz, S. Martorell, Intercomparison of full energy peak efficiency curves for an HPGe detector using MCNP6 and GEANT4, *J. Radiat. Phys. Chem.* 155 (2019) 248–251.
- [6] K. Huang, J.L. Dai, C.Q. Xu, Z. Yi, L.F. Meng, Magnetic flux signal extraction method based on wavelet threshold filtering, *IOP Conf. Ser. Earth Environ. Sci.* 237 (3) (2019) 20–32.
- [7] J.H. Cai, Gear fault diagnosis based on a new wavelet adaptive threshold denoising method, *Ind. Lubric. Tribol.* 71 (1) (2019) 40–47.
- [8] Y.Y. Luo, L.Q. Ge, C. Xiong, F.Q. Chen, Smoothing technology of gamma-ray spectrometry data based on matched filtering, *J. Nucl. Electron. Detect. Technol.* 33 (1) (2013) 107–109.
- [9] A. Peter Gorry, General least-squares smoothing and differentiation by the convolution(Savitzky–Golay) method, *Anal. Chem.* 62 (6) (2002) 570–573.
- [10] H.B. Lu, X. Li, I.T. Hsiao, Z.G. Liang, Analytical noise treatment for lowdose CT projection data by penalized weighted least-square smoothing in the K-L domain, *Chin. J. Med. Phys.* 19 (4) (2002) 200–204.
- [11] X. Sun, N. He, Y.Q. Zhang, X.Y. Zhen, K. Lu, X.L. Zhou, Color image denoising based on guided filter and adaptive wavelet threshold, *Appl. Comput. Intell. Soft Comput.* (2017) 1–11.
- [12] J.J. Liang, J. Zhao, Y.X. Hao, An image denoising and enhancement algorithm for inner and outer ring of wavelet bearings based on improved threshold, *J. Phys. Conf.* 1069 (2018).
- [13] J.M. Fu, Y.F. Li, Image denoising based on wavelet transform and improved threshold function, in: 2017 2nd International Conference on Electrical and Electronics: Techniques and Applications (EETA2017), 2017, pp. 346–350.
- [14] W. Jenkal, R. Latif, A. Toumanari, A. Dliou, An efficient algorithm of ECG signal denoising using the adaptive dual threshold filter and the discrete wavelet transform, *Biocybern. Biomed. Eng.* 36 (3) (2016) 499–508.
- [15] Agnihotri Kumar, Biosignal denoising via wavelet thresholds, *IETE J. Res.* (2010) 132–138.
- [16] Y. Zhang, W.F. Ding, Z.F. Pan, J. Qin, Improved wavelet threshold for image Denoising, *Front. Neurosci.* 2 (2019) 13–39.
- [17] Q. Lu, L.X. Pang, H.Q. Huang, C. Shen, H.L. Cao, Y.B. Shi, J. Liu, High-G calibration denoising method for high-G MEMS accelerometer based on EMD and wavelet threshold, *Micromachines* 10 (2) (2019) 134.
- [18] H.W. Duan, S.S. Ma, L.J. Han, G.Q. Huang, A novel denoising method for laser-induced breakdown spectroscopy: improved wavelet dual threshold function method and its application to quantitative modeling of Cu and Zn in Chinese animal manure composts, *Microchemical J.* 134 (2017) 262–269.
- [19] Z.D. Yan, G. Chen, W.Y. Xu, C.M. Yang, Y. Lu, Study of an image autofocus method based on power threshold function wavelet reconstruction and a quality evaluation algorithm, *Appl. Optic.* 57 (33) (2018) 9714–9721.
- [20] F.K. Zhao, A.M. Wang, A background removing approach based on complex wavelet transform for X-ray fluorescence spectrometry, *Metall. Anal.* 35 (7) (2015) 10–14.
- [21] L.H. Li, J.F. He, Q. Wang, Y. Wang, Study of γ energy spectrum denoising based on improved wavelet threshold method, *J. Atom. Energy Sci. Technol.* 50 (7) (2016) 1279–1283.
- [22] Y.Z. Chen, Y.W. Wang, W. Yang, Y. Liu, Wavelet denoising algorithm based on a new threshold function, *Commun. Technol.* 50 (7) (2017) 1407–1411.
- [23] R.S. Li, B. He, G.Z. Fu, J. Li, The wavelet transform and its application in the denosing manipulation of γ spectrum, *Chin. J. Nucl. Sci. Eng.* 27 (2) (2017) 187–191.
- [24] R. Su, Z.Q. Wang, Research of wavelet de-noising control for γ spectrum, *Atomic Energy Sci. Technol.* 48 (7) (2014) 1309–1313.
- [25] C.H. Zeng, X.J. Feng, Z.S. Duan, B. Qun, Y. Wu, Processing and analysis of γ energy spectrum data based on modulus maximum method, *Atomic Energy Sci. Technol.* 51 (7) (2017) 1305–1310.
- [26] Y.C. Yan, M.Z. Liu, F.Z. Liu, Study of smooth processing to γ energy spectrum by using an average wavelet threshold method, *Nucl. Phys. Rev.* 31 (3) (2014) 407–410.
- [27] P.C.L. Da Silva, J.P. Da Silva, A.R.G. Garcia, Daubechies wavelets as basis functions for the vectorial beam propagation method, *J. Electromagn. Waves Appl.* 33 (8) (2019) 1027–1041.
- [28] V. Vineet, M. Siddhartha, P.T. Akhilanand, Multiscale subspace identification of nuclear reactor using wavelet basis function, *Ann. Nucl. Energy* 111 (2018) 280–292.
- [29] Y.D. Gao, H.L. Wang, S.H. You, L. Feng, Y.Y. He, K. Liu, Research on pulsar signal denoising algorithm based on wavelet basis function selection and improved threshold function, *Electron. Optic. Contr.* 6 (2019). <http://kns.cnki.net/kcms/detail/41.1227.TN.20190621.0919.002.html>.
- [30] D.L. Donoho, De-noising by soft-thresholding, *IEEE Trans. Inf. Theor.* 41 (3) (1995) 613–627.
- [31] D.L. Donoho, I.M. Johnston, Adapting to unknown smoothness via wavelet shrinkage, *J. Am. Stat. Assoc.* 90 (432) (1995) 1200–1224.